# Bi-layered Composite Scaffold for Repair of the Osteochondral Defects

Dongdong Xu,[1,2,*] Gu Cheng,[1,*] Jinhong Dai,[1,2] and Zhi Li[1,†]

[1]*The State Key Laboratory Breeding Base of Basic Science of Stomatology (Hubei-MOST) and the Key Laboratory of Oral Biomedicine Ministry of Education, and Department of Oral and Maxillofacial Surgery, School and Hospital of Stomatology, Wuhan University, Wuhan, People's Republic of China.*

[2]*The Department of Oral and Maxillofacial Surgery, School and Hospital of Stomatology, Wenzhou Medical University, Wenzhou, People's Republic of China.*

**These two authors contributed equally to this work.*

**Zhi Li, PhD**

Submitted for publication December 10, 2019. Accepted in revised form October 19, 2020.

†Correspondence: The State Key Laboratory Breeding Base of Basic Science of Stomatology (Hubei-MOST) and the Key Laboratory of Oral Biomedicine Ministry of Education, and Department of Oral and Maxillofacial Surgery, School and Hospital of Stomatology, Wuhan University, 237 Luoyu Road, Wuhan 430079, People's Republic of China
(e-mail: zhili@whu.edu.cn).

**Objective:** Osteochondral defect presents a big challenge for clinical treatment. This study aimed at constructing a bi-layered composite chitosan/chitosan-$\beta$-tricalcium phosphate (CS/CS-$\beta$-TCP) scaffold and at repairing the rat osteochondral defect.

**Approach:** The bi-layered CS/CS-$\beta$-TCP scaffold was fabricated by lyophilization, and its microstructure was observed by a scanning electron microscope. Chondrocytes and bone marrow stem cells (BMSCs) were seeded into the CS layer and the CS-$\beta$-TCP layer, respectively. Viability and proliferation ability of the cells were observed under a confocal microscope. After subcutaneous implantation, the chondrogenic ability of the CS layer and osteogenic ability of the CS-$\beta$-TCP layer were evaluated by immunofluorescence. Then, the bi-layered scaffolds were implanted into the rat osteochondral defects and the harvested samples were macroscopically and histologically evaluated.

**Results:** The bi-layered CS/CS-$\beta$-TCP scaffold exhibited the distinctive microstructures for each layer. The seeded chondrocytes in the CS layer could maintain the chondrogenic lineage, whereas BMSCs in the CS-$\beta$-TCP layer could continually differentiate into the osteogenic lineage. Moreover, cells in both layers could maintain well viability and excellent proliferation ability. For the *in vivo* study, the newly formed tissues in the bi-layered scaffolds group were similar with the native osteochondral tissues, which comprised hyaline-like cartilage and subchondral bone, with better repair effects compared with those of the pure CS group and the blank control group.

**Innovation:** This is the first time that the bi-layered composite CS/CS-$\beta$-TCP scaffold has been fabricated and evaluated with respect to osteochondral defect repair.

**Conclusion:** The bi-layered CS/CS-$\beta$-TCP scaffolds could facilitate osteochondral defect repair and might be the promising candidates for osteochondral tissue engineering.

**Keywords:** osteochondral defect, bi-layered scaffold, $\beta$-tricalcium phosphate, chitosan

## INTRODUCTION

Osteochondral defects caused by osteoarthritis or traumatic injuries can bring about joint deformity, limited mobility of joints, and significant pain.[1] Because cartilage tissue exhibits lack of vascularization and the metabolic activity of mature chondrocytes is limited, self-repair is difficult after injury.[2] The current existing clinical treatments for osteochondral defect, including



DOI: 10.1089/wound.2019.1140

arthroscopic debridement,[3] artificial joint replacement,[4] chondral and osteochondral grafts,[5–7] and bone marrow stimulation,[8–10] have disadvantages such as donor-site morbidity, anatomical mismatching, pain, and infection.[5] In recent years, tissue-engineered scaffolds have been widely utilized to treat the osteochondral defects.

Osteochondral defect involves the articular cartilage and the subchondral bone defect, with different biological and mechanical properties. Therefore, it is necessary for us to design a bi-layered tissue-engineered scaffold to mimic the anatomical and physiological hierarchical structures of the native osteochondral tissues.[11] Bi-layered scaffold provides a transition region between the bone and cartilage layer and a platform with those two kinds of tissue grown in it at the same time. Currently, fabrication of bi-layered scaffolds for osteochondral defect repair is still a challenge, because each layer of the scaffold should possess tissue-special biological and mechanical properties to support regeneration of two distinct but integrated tissues. Several bi-layered scaffolds for osteochondral defect repair have been investigated in previous studies.[12–17] Kim *et al.*[14] fabricated a bi-layered scaffold comprising PLGA/$\beta$-TCP (for bone layer) and PLCL (for cartilage layer) by combining a sintering method and a gel pressing method. Galperin *et al.*[12] applied a sphere-templating technique to fabricate a bi-layered scaffold based on degradable poly(hydroxyethyl methacrylate) hydrogel, in which one layer was designed with a single defined, monodispersed pore size of 38 $\mu$m and pore surfaces coated with hydroxyapatite particles to promote regrowth of subchondral bone whereas the second layer had 200 $\mu$m pores with surfaces decorated with hyaluronan for articular cartilage regeneration. The two scaffolds showed different biological and mechanical properties of each layer, but their fabrication technologies were complex and their applications and repairing effects for osteochondral defect were not performed. In this work, an easily fabricated bi-layered chitosan/chitosan-$\beta$-tricalcium phosphate (CS/CS-$\beta$-TCP) scaffold was designed, in which CS acted as a cartilage layer and CS-$\beta$-TCP as a bone layer, and its application in rat osteochondral defect was evaluated.

CS, a natural polymer, has been widely used as one of the scaffold materials for tissue engineering because of its excellent biocompatibility, biodegradability, nontoxicity, and antibacterial and porous structure.[18–20] As a linear polysaccharide, CS consisted of $\beta(1 \rightarrow 4)$ linked D-glucosamine residues with a variable number of randomly located *N*-acetyl-glucosamine groups. The structure of CS is similar with various glycosaminoglycan and hyaluronic acid, which is the main matrix of cartilage.[21] A previous study proved that chondrocytes that were seeded on CS films could continue to express collagen type II and aggrecan after 7 days of culture.[22] In addition, the porous CS-based scaffolds could support attachment of chrondrocytes and maintain their cellular morphology. After 18 days of cells inoculation, proteoglycan and type II collagen (Col-II) were detected in cartilaginous extracellular matrix (ECM).[23] Based on the earlier mentioned contents, it is safely concluded that CS could be an ideal scaffold material for cartilage tissue engineering.

$\beta$-TCP is a biocompatible and bioactive material for bone tissue engineering. It can directly bind to natural bone tissues, then be absorbed, and gradually replaced by newly formed bone tissue.[24] To overcome the disadvantage of the inorganic ceramic material, $\beta$-TCP is often combined with other organic biopolymer materials.[25] It has been proved that scaffolds with $\beta$-TCP and CS can not only promote the adhesion and proliferation[25–27] but also promote the osteogenic differentiation of osteoblasts and bone marrow stem cells (BMSCs).[26,27]

Therefore, the bi-layered composite scaffold with CS acted as a cartilage layer and CS-$\beta$-TCP as a bone layer was fabricated in this study. To examine the potential of the bi-layered scaffold for osteochondral regeneration, *in vitro* and *in vivo* experiments were performed.

## CLINICAL PROBLEM ADDRESSED

Osteochondral defects caused by osteoarthritis or traumatic injuries are difficult to repair, because cartilage tissue exhibits a lack of vascularization and the defects involve the articular cartilage and the subchondral bone, which are two tissues with different biological and mechanical properties. Currently, the most commonly used clinical treatments for osteochondral defect is autologous osteochondral grafts.[5] However, the autograft harvested from a nonload-bearing area still presents problems such as donor-site morbidity and anatomical mismatching. Osteochondral tissue engineering offers an alternative with the potential to overcome the problems just mentioned. The critical point of osteochondral tissue engineering is to promote individual growth of cartilage and bone tissues simultaneously in a scaffold. Therefore, the objective of this study is to construct and fabricate a bi-layered composite CS/CS-$\beta$-TCP scaffold that can provide a platform with those two kinds of

tissue grows in it at the same time and facilitate the translation of laboratory research results into clinical application.

## MATERIALS AND METHODS

### Preparation of the bi-layered CS/CS-β-TCP scaffold

Solution A was prepared by adding CS power (Aladdin, Shanghai, China) dissolved in 2% acetic acid and adjusting the final concentration of CS to 1% w/v. Solution B was made by dissolving β-TCP powder into Solution A and stirring for 24 h. Solution B was put into a 48-well polystyrene plate (0.3 mL/well), and then the 48-well polystyrene plate was frozen for 8 h at –80°C. Solution A was precooled at 4°C for 2 h and then poured onto the surface of the Solution B-layer (0.3 mL/well) followed by freezing at –80°C for 12 h. After another 48 h of freezing at –80°C, the bi-layered composite CS/CS-β-TCP scaffolds were freeze-dried for 24 h and removed from the molds (Fig. 1a). For the *in vivo* experiment, to match the size of the osteochondral defect in rats, the mono-layered CS scaffolds and bi-layered CS/CS-β-TCP scaffolds were cut out from the fabricated CS/CS-β-TCP scaffolds (Fig. 1b).

### Characterization of the composite scaffolds

The morphology of the bi-layered composite CS/CS-β-TCP scaffolds was examined by a scanning electron microscope (SEM; Zeiss SIGMA, German). Before the microscopy, the scaffold samples were coated with gold by using a sputter coater.

The porosities of the pure CS and CS-β-TCP single-phase scaffold separated from a CS/CS-β-TCP scaffold were measured by the liquid displacement method.[28] Briefly, a CS/CS-β-TCP scaffold was cut into two half-blocks from the connection of the two phases between CS and CS-β-TCP layers. Each half block was immersed in a graduated cylinder containing a certain volume (V1) of ethanol for 5 min. Then, a series of brief evacuation–repressurization cycles were conducted to force the ethanol into the pores of the scaffolds until no air bubbles were squeezed out from the scaffold. Then, the total volume of ethanol with the ethanol-impregnated scaffold inside was recorded as V2. The volume of the residual ethanol was recorded as V3 after the ethanol-impregnated scaffold was removed. The porosity of the scaffold was calculated by: Porosity (%) = (V1 – V3)/(V2 – V3) × 100%. The values were expressed as mean ± standard deviation ($n = 3$).

### Isolation and culture of seeded cells

*Isolation and culture of chondrocytes.* All animal experimental protocols were approved by the Animal Care and Use Committee of Wuhan University. Chondrocytes were isolated from the knee joint articular cartilages of 24-h-old Sprague-Dawley (SD) rats by using the enzymatic digestion method with slight modifications.[29] Briefly, the cartilage was minced and washed twice in phosphate-buffer solution (PBS; Hyclone) supplemented with 1% penicillin–streptomycin (P-S; Hyclone). Then, the cartilage was digested by 0.05% (w/v) type II collagenase (Solarbio, Beijing, China) solution under shaking for 8 h at 37°C. After digestion, the cartilage fragments were incubated in Dulbecco's modified Eagle medium/Nutrient Mixture Ham-12 (DMEM/F12; Hyclone) containing 10% fetal bovine serum (FBS, Hyclone, New Zealand) and 1% P-S at 37°C in a humidified atmosphere containing 5% $CO_2$. After 24 h of culture, the cartilage fragments were removed through changes of medium and the attached chondrocytes were further expanded in new

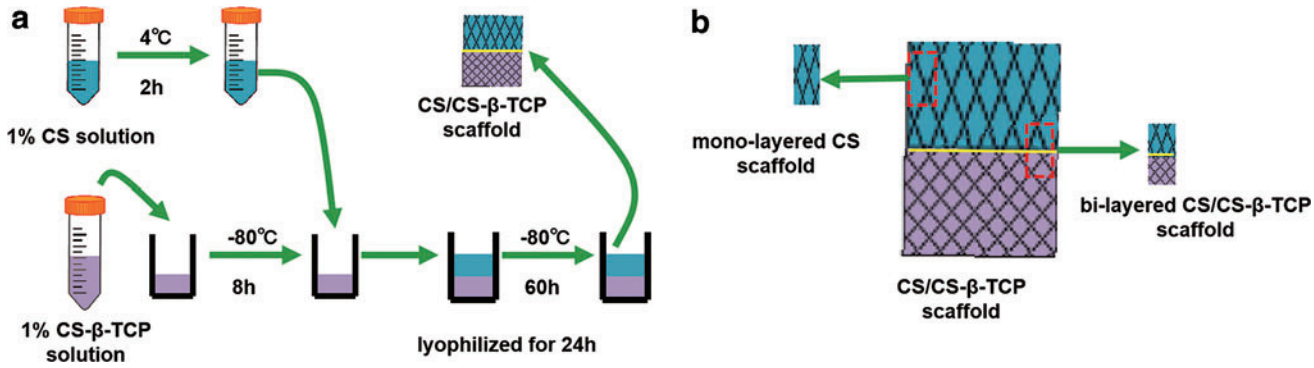


**Figure 1.** Fabrication process of bi-layered CS/CS-β-TCP scaffold **(a)**. For the *in vivo* experiment, the mono-layered CS and bi-layered CS/CS-β-TCP scaffolds were cut out from the fabricated CS/CS-β-TCP scaffolds **(b)**. CS/CS-β-TCP, chitosan/chitosan-β-tricalcium phosphate. Color images are available online.

culture medium. The second passage cells were used in the following experiments.

*Isolation and culture of BMSCs.* BMSCs were isolated from bone marrow of 6-week-old SD rats, as preciously described with minor modifications.[30] Briefly, the femurs and tibias of rats were cut at both metaphyseal ends and the bone marrow was flushed out with PBS by using a sterile syringe. After obtaining the bone marrow solution, the concentrated buffy coat was separated from red cells by centrifugation at 2,000 rpm for 20 min. The obtained cells were cultured in DMEM/F12 supplemented with 10% FBS and 1% P-S at 37°C in a humidified atmosphere containing 5% $CO_2$. Two days after isolation, the culture medium was changed, and nonadherent cells were removed by rinsing three times with PBS. After 80–90% confluence of cells was attained, the BMSCs were passaged. The BMSCs obtained from the third passage[31] were used in the following experiments.

### Cell labeling

The second chondrocytes were labeled with CFSE dye[16] with a green color (Beyotime, China) according to the manufacturer's protocol. Briefly, 10 $\mu$L sterile stock solution of CFSE dye (2 mM solution) was added to 4 mL cells suspension with a total number of $1 \times 10^6$ cells. The dye was allowed to be in contact with the chondrocytes for 30 min at 37°C. The cells were rinsed three times in PBS to remove all unbound CFSE dyes.

Also, the BMSCs were labeled with the red fluorescent dye CM-DiI (Sigma).[30] In brief, a 10 $\mu$L sterile stock solution of CM-DiI (2 mM solution) was added to a 10 mL cells suspension of $1 \times 10^6$ cells. The dye was allowed to be in contact with the BMSCs for 5 min at 37°C and for another 15 min at 4°C. The cells were rinsed three times in PBS to remove all unbound CM-DiI dyes.

### Cell distribution and proliferation in the scaffold

All scaffolds were sterilized by ethylene oxide, completely washed with PBS three times (30 min each time), and finally immersed in DMEM/F12 for 24 h until they were used. Before cell seeding, scaffolds were dried on the filter paper. Then, 100 $\mu$L chondrocytes suspension with a density of $1 \times 10^6$ cells/mL were seeded into the CS layer of the CS/CS-$\beta$-TCP scaffold with a microliter syringe and 100 $\mu$L BMSCs suspensions with the same density were seeded into the CS-$\beta$-TCP layer. The cell-seeded scaffolds were precultured for 2 h at 37°C in a humidified atmosphere containing 5% $CO_2$ before immersion of cells/scaffold composites in complete medium.

The distribution of chondrocytes and BMSCs seeded inside the scaffold were observed under a confocal laser scanning microscope (CLSM) at 1, 7, and 14 days of seeding. To analyze the cell proliferation in the scaffold, three different slides of each layer at different depths were chosen, the labeled cells were counted by using ImageJ software, and three scaffolds were used at each time point. Before being visualized under CLSM, the scaffolds were taken out from culture plates and rinsed with PBS gently.

### Cell viability assessment

Live/Dead Cell Vitality Assay Kit (Molecular Probes) was used to evaluate the viability of cells attached on the composite scaffolds according to the manufacturer's instructions.[32] Cells without fluorescent dye labeling were seeded into the scaffolds. After being incubated for 14 days, each scaffold was washed with PBS for 3 min and then incubated in 500 $\mu$L Live/Dead staining solution containing 2 $\mu$M calcein-AM (green dye for live cells) and 6 $\mu$M ethidium homodimer-1 (red dye for dead cells) reagents for 30 min at 37°C. The scaffolds were observed under CLSM with 488 and 568 nm excitation.

### Subcutaneous implantation experiments

For subcutaneous implantation, six 9-week-old nude mice (Hubei Provincial Laboratory Animal Center, China) were used. General anesthesia was administered with 0.3% pentobarbital sodium (around 2.3 mL/kg body weight; Sigma). Subcutaneous incisions of $\sim$1 cm were made on the back skin of nude mice. The bi-layered CS/CS-$\beta$-TCP scaffolds with chondrocytes and BMSCs seeded in each layer were implanted subcutaneously ($n = 6$).

After 3 and 6 weeks of implantation, the nude mice were euthanized by $CO_2$ inhalation and the implants were harvested and cut into CS layers and CS-$\beta$-TCP layers from the connection. All the fixed samples were fixed in 10% (v/v) buffered formalin, dehydrated in a graded ethanol series, then embedded in paraffin, and finally cut into 6-$\mu$m-thick sections. The immunofluorescence staining of Col-II was performed on CS layers. Subsequently, a 1% bovine serum albumin solution was dropped to the sections and blocked at 37°C for 30 min. Thereafter, the samples were incubated overnight with primary antibodies against Col-II (1:100; Abcam) and subsequently with a Cy3-labeled secondary antibody (1:50; Aspen) at 37°C for 1 h. For CS-$\beta$-TCP layers, the immunofluorescence staining of osteocalcin (OCN) was performed. After

blocking, the samples were incubated overnight with primary antibodies against OCN (1:100; Abcam) and subsequently with an FITC-labeled secondary antibody (1:50; Aspen) at 37°C for 1 h. The immunofluorescence staining of type I collagen (Col-I) was performed on both CS and CS-$\beta$-TCP layers. The samples were incubated overnight with primary antibodies against Col-I (1:100; Sigma) and subsequently with a AlexaFluor® 594-labeled secondary antibody (1:200; Abcam) at 37°C for 1 h. After staining, the slides were photographed by using fluorescence microscopy, the images were analyzed by the ImageJ software, and three slides of every specimen were used at each time point.

### *In vivo* experiments

*Animal model.* Forty-eight adult male SD rats (280–300 g) (Hubei Provincial Laboratory Animal Center) were randomly divided into three groups, each comprising 16 rats: a control group, a CS group, and a CS/CS-TCP group. All animals were housed at the SPF animal laboratory for 1 week before the operation.

Articular defects were made according to a previous study.[30] After general anesthesia by 0.3% pentobarbital sodium (around 2.3 mL/kg body weight; Sigma), a 10-mm-long medial prepatellar skin incision was made on the skin of the right leg, and the knee joint was exposed further via lateral dislocation of the patella. An osteochondral defect (1.5 mm in diameter and 3.0 mm in depth) in the trochlear groove of the femur was created by a dental high-speed turbine drill. The defects in the rats were treated with different kinds of scaffolds with diameter of 1.5 mm and height of 3.0 mm. The defects without any treatment were used as blank control. After surgery, the rats were allowed to move freely in their cages.

*Histological examination.* After 6 and 12 weeks of surgery, the animals were sacrificed and the dissected distal femurs were examined grossly by a stereomicroscope (SMZ-10; Nikon, Tokyo, Japan). To evaluate the newly formed cartilaginous tissues in the defects, a previously developed scale method (Table 1)[33] was used to grade the newly formed tissues blindly by three observers at 12 weeks after operation. The harvested samples of 12 weeks were investigated by using micro-computed tomography (CT; Scanco Medical AG, Bassersdorf, Switzerland), and the percentage of newly formed bone of the defects was then calculated.

After all the fixed samples were decalcified in 10% EDTA solution (pH = 7.5), dehydrated, and embedded in paraffin for histological analyses, the 5 $\mu$m sections at the defect site were cut sagittally and prepared for hematoxylin and eosin (HE) and Masson staining. All histological sections were observed with a light microscope (Olympus, Japan). The International Cartilage Repair Society (ICRS) Visual Histological Assessment Scale (Table 2)[33] was used to grade the repaired tissues blindly by three observers at 12 weeks after operation.

**Table 1.** *Macroscopic grading scale of cartilage repair*

| *Feature* | *Points* |
|---|---|
| Coverage | |
| >75% fill | 4 |
| 50–75% fill | 3 |
| 25–50% fill | 2 |
| <25% fill | 1 |
| No fill | 0 |
| Neocartilage color | |
| Normal | 4 |
| 25% yellow/brown | 3 |
| 50% yellow/brown | 2 |
| 75% yellow/brown | 1 |
| 100% yellow/brown | 0 |
| Defect margins | |
| Invisible | 4 |
| 25% circumference visible | 3 |
| 50% circumference visible | 2 |
| 75% circumference visible | 1 |
| Entire circumference visible | 0 |
| Surface | |
| Smooth/level with normal | 4 |
| Smooth but raised | 3 |
| Irregular 25–50% | 2 |
| Irregular 50–75% | 1 |
| Irregular >75% | 0 |

**Table 2.** *International Cartilage Repair Society visual histological evaluation of cartilage repair*

| *Feature* | *Points* |
|---|---|
| Surface | |
| Smooth/continuous | 3 |
| Discontinuities/irregularities | 0 |
| Matrix | |
| Hyaline | 3 |
| Mixture: hyaline/fibrocartilage | 2 |
| Fibrocartilage | 1 |
| Fibrous tissue | 0 |
| Cell distribution | |
| Columnar | 3 |
| Mixed/columnar clusters | 2 |
| Clusters | 1 |
| Individual cells/disorganized | 0 |
| Viability of cell population | |
| Predominantly viable | 3 |
| Partially viable | 1 |
| <10% viable | 0 |
| Subchondral bone | |
| Normal | 3 |
| Increased remodeling | 2 |
| Bone necrosis/granulation tissue | 1 |
| Detached/fracture/callus at base | 0 |

For detailed immunohistochemical examination, sections were incubated with 3% $H_2O_2$ to quench the endogenous peroxidase activity followed by rinsing in PBS for 5 min. After blocking with 1.5% rabbit serum for 20 min, the sections were incubated overnight at 4°C with primary antibodies against Col-I (1:200; Affinity Biosciences) and Col-II (1:200; Affinity Biosciences), in accordance to the manufacturer's instructions. Subsequently, the sections were incubated with horseradish peroxidase-conjugated secondary antibodies (Bio-Swamp, China) at room temperature for 30 min. Finally, the nuclei were counterstained with hematoxylin and histological sections were observed under a light microscope (Olympus).

### Statistical analysis

The data were presented as the mean ± standard deviation and analyzed by one-way analysis of variance using SPSS 17.0 software. A $p$-value of $<0.05$ was considered statistically significant.

## RESULTS

### Characterization of the bi-layered scaffolds

The CS layer of the CS/CS-$\beta$-TCP scaffold was looser compared with the CS-$\beta$-TCP layer (Fig. 2a, b). Further, the interface region of the two layers was apparent (Fig. 2c). The SEM images also showed that the interface of the two layers was well attached with each other (Fig. 2f). The pore size of the CS layer (120–400 $\mu$m) (Fig. 2d) was larger than that of the CS-$\beta$-TCP layer (10–80 $\mu$m) (Fig. 2e). The porosity of the CS layer (75.3% ± 2.4%) was comparable with that of the CS-$\beta$-TCP layer (77.2% ± 2.6%) ($p > 0.05$).

### Cells distribution and viability

As shown in Fig. 3, the scaffolds exhibited a blue color because of their auto-fluorescence.[34] Chondrocytes and BMSCs were distributed in the CS layer (Fig. 3a–c) and CS-$\beta$-TCP layers (Fig. 3d–f), respectively. In the interface region between the two layers, a few chondrocytes and BMSCs have penetrated into different layers for each other after 14 days of incubation (Fig. 3h).

The Live/Dead staining was performed to evaluate the cell viability after 14 days of incubation. The results showed that 96.2% ± 2.5% of chondrocytes in the CS layer and 95.2% ± 3.3% of BMSCs in the CS-$\beta$-TCP layer of the scaffold kept alive and exhibited a green color.

### Immunofluorescence evaluation

The osteogenic and chondrogenic capacity of the bi-layered CS/CS-$\beta$-TCP scaffolds with BMSCs and chondrocytes seeded in each layer were evaluated after 3 and 6 weeks of subcutaneous implantation. There was no sign of infection or swelling observed during the entire experimental period (Fig. 4j).

The expression of Col-II, a major component of the ECM and synthesis products of chondrocytes in hyaline cartilage,[12] was examined by immunofluorescence staining to evaluate the chondrogenic ability of chondrocytes in the CS cartilage layer.

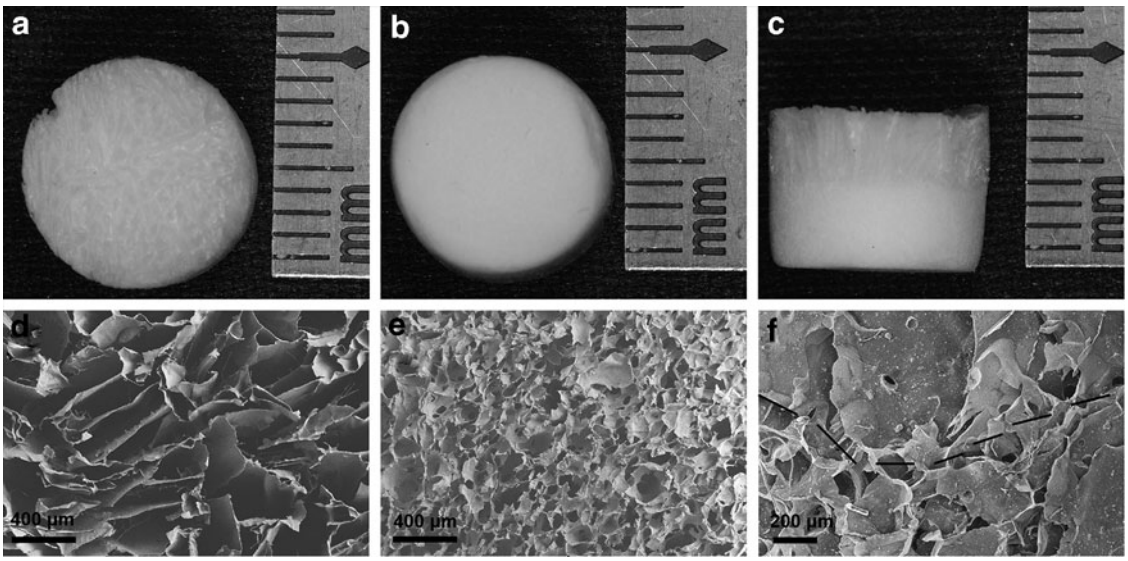


**Figure 2.** Macroscopic and microscopic structures of the CS/CS-$\beta$-TCP scaffold. The gross appearance of the CS layer and CS-$\beta$-TCP layer **(a–c)**. The SEM image of the CS layer **(d)**, CS-$\beta$-TCP layer **(e)**, and their interface region **(f)**. The *black dotted line* is used to label the interface of the two layers **(f)**. SEM, scanning electron microscope.

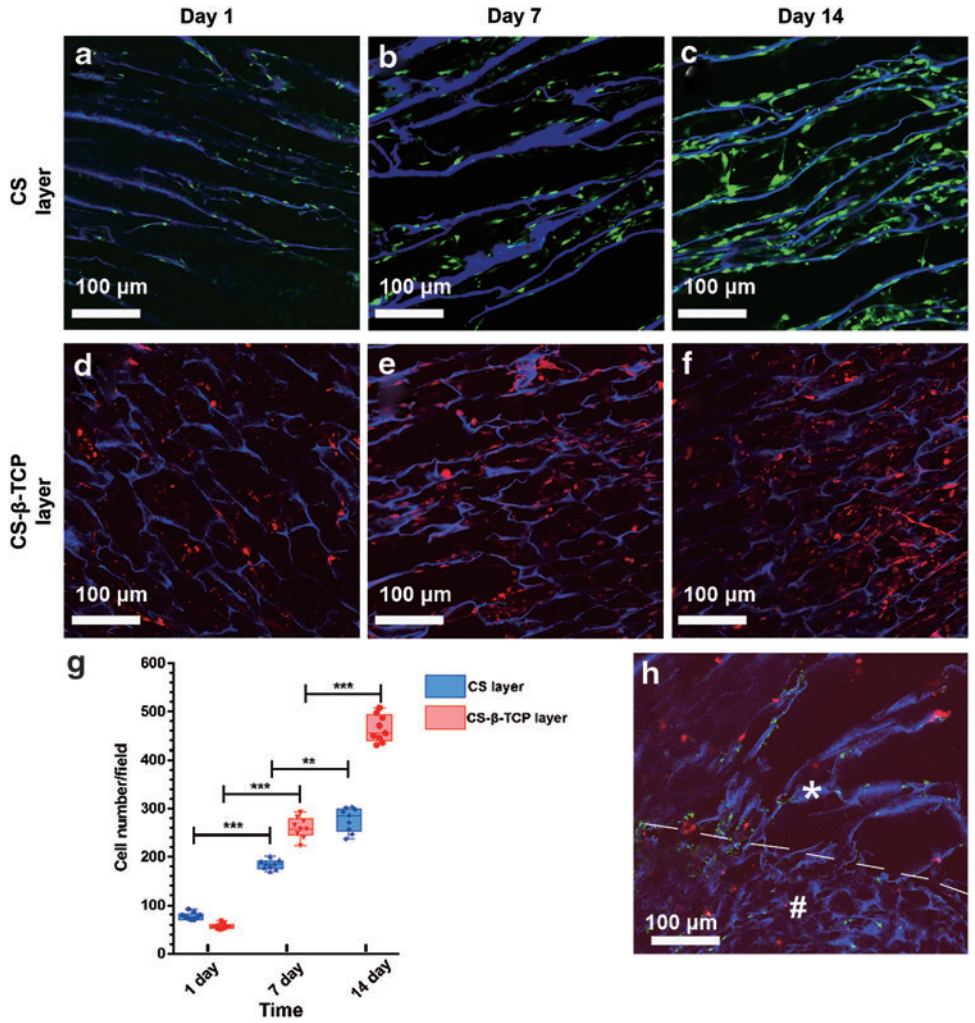


**Figure 3.** Confocal images of cell distribution in the scaffolds after 1, 7, and 14 days of culture. Chondrocytes were stained with CFSE (*green*) in the CS layer **(a–c)**, and BMSCs were stained with CM-DiI (*red*) in the CS-$\beta$-TCP layer **(d–f)**. The interface between CS and CS-$\beta$-TCP layers after 14 days of culture was shown in **(h)**. The *white* "*" represents the CS layer, the *white* "#" represents the CS-$\beta$-TCP layer, and the white dotted line is used to label the interface of the two layers. **(g)** Shows the mean cells number of each observation field. Data represent mean ± standard deviation; $^{**}p<0.01$, $^{***}p<0.001$. BMSCs, bone marrow stem cells. Color images are available online.

At 3 weeks of implantation, Col-II immunofluorescence staining demonstrated a positive reaction and exhibited a red color. Till the 6 weeks of implantation, the expression of Col-II was a little stronger than that of 3 weeks ($p<0.01$) (Fig. 4a, b, k).

The OCN was examined to evaluate the osteogenic capacity of BMSCs in the CS-$\beta$-TCP bone layer. Positive staining of OCN was observed in the cells of the CS-$\beta$-TCP layer and exhibited a green color at 3 weeks of implantation. Till 6 weeks of implantation, OCN expression in the cells of the CS-$\beta$-TCP layer was a little stronger than that of 3 weeks ($p<0.05$) (Fig. 4e, f, k).

Col-I, a component of the ECM, is a critical marker of fibrocartilage formation.[30] Almost no Col-I was expressed in the CS cartilage layer at both 3 and 6 weeks of implantation (Fig. 4c, d), whereas the Col-I expression in the CS-$\beta$-TCP bone layer was obvious at both 3 and 6 weeks of implantation (Fig. 4g, h). Moreover, the Col-I expression in the CS-$\beta$-TCP layer was significantly higher than that in the CS cartilage layer ($p<0.001$) (Fig. 4l).

### Macroscopic observation

All the animals used in this study survived the entire period of *in vivo* experiments. There was no sign of infection or swelling observed in the defect sites. At 6 weeks after operation, the defects in the blank control group were still unfilled, as nearly no new tissue formed in the defect sites (Fig. 5i). The surface of the defect sites in the CS group was rough, and the margins around the defect sites were still obvious (Fig. 5a). As to the CS/CS-$\beta$-TCP

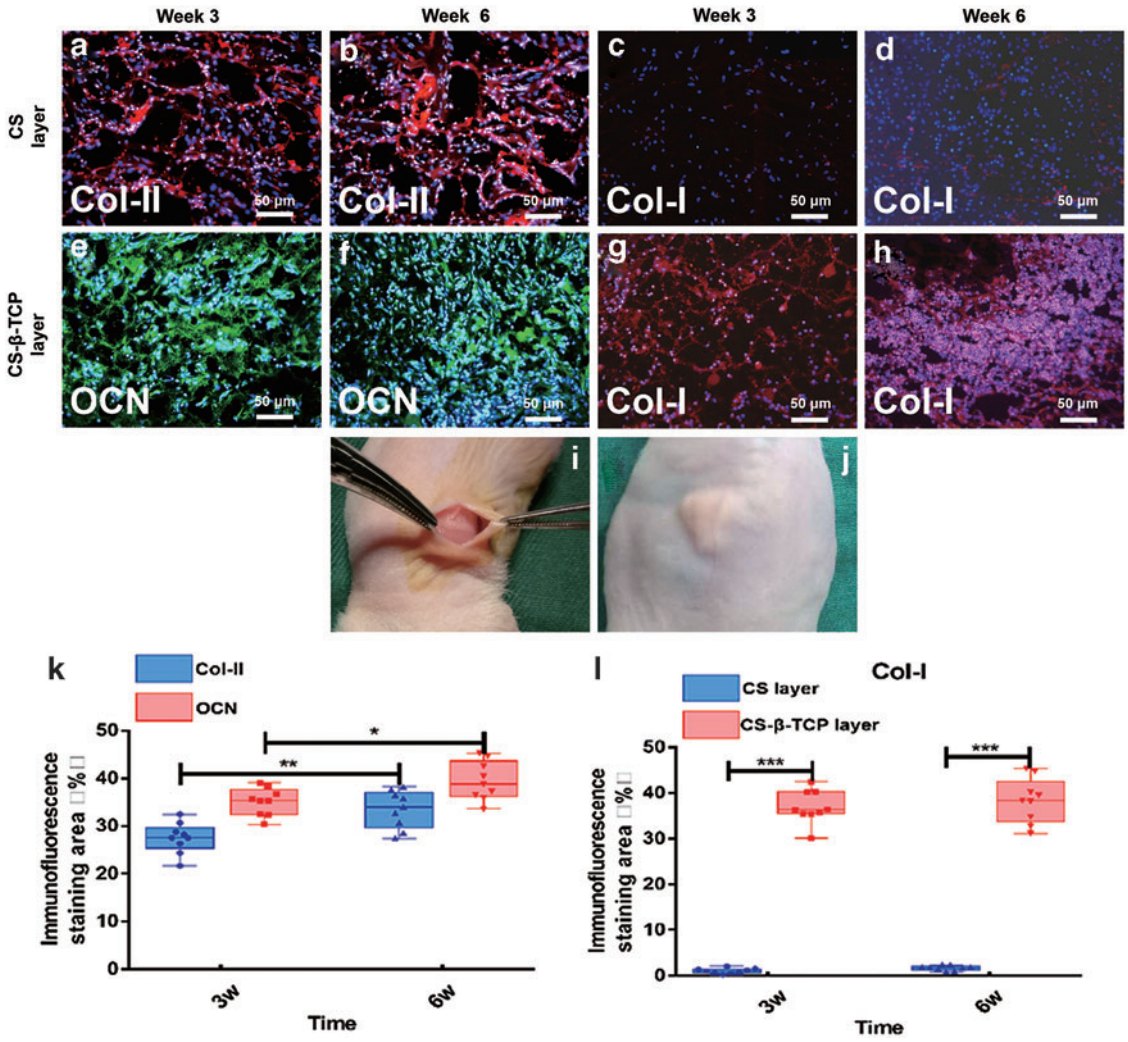


**Figure 4.** Subcutaneous implantation experiments were performed **(i)**. The immunofluorescence staining of Col-II in the CS layers at 3 weeks **(a)** and 6 weeks **(b)** after implantation (*Red:* positive for Col-II, *blue:* DAPI for nucleus). The immunofluorescence staining of OCN in the CS-$\beta$-TCP layers at 3 weeks **(e)** and 6 weeks **(f)** after implantation (*Green:* positive for OCN, *blue:* DAPI for nucleus). The immunofluorescence staining of COL-I in the CS layers and CS-$\beta$-TCP layers at 3 weeks **(c, g)** and 6 weeks **(d, h)** after implantation (*Red:* positive for Col-I, *blue:* DAPI for nucleus). The intensity of immunofluorescence staining (%) of Col-II, OCN, **(k)** and Col-I **(l)** was semi-calculated by ImageJ software. Data represent mean ± standard deviation; *$p<0.05$, **$p<0.01$, ***$p<0.001$. Col-I, type I collagen; Col-II, type II collagen; OCN, osteocalcin. Color images are available online.

group, the newly formed tissues were smooth and the margins became vague at 6 weeks of operation (Fig. 5e).

At 12 weeks after operation, the defect sites in the CS/CS-$\beta$-TCP group were filled with cartilage-like tissues and almost completely repaired. The newly formed cartilaginous tissues integrated well with the surrounding native cartilage, and there were no obvious margins (Fig. 5f). In the CS group, the surface cartilage was still rough and exhibited a distinctive morphology with the host cartilage (Fig. 5b). In the blank control group, all the defects failed to repair and the defects were still concave (Fig. 5j). The macroscopic grading scale of the three groups is shown in Table 3; the total score of the bi-layered CS/CS-$\beta$-TCP group was significantly higher than that of the mono-layered CS group and the blank group ($p<0.001$).

## Micro-CT observation

Micro-CT scanning was performed to evaluate the formation of subchondral bone (Fig. 5c, g, k). Conforming to the results of macroscopic observation, the subchondral bone defects in the CS group and blank group were unrepaired at 12 weeks of operation. However, the defects in the CS/CS-$\beta$-TCP group were almost repaired and the margin between scaffolds and the native tissue was vague (Fig. 5g). The percentage of the newly formed bone in the defects was significantly larger than that of the mono-layered CS group and the blank group ($p<0.001$) (Fig. 5l).

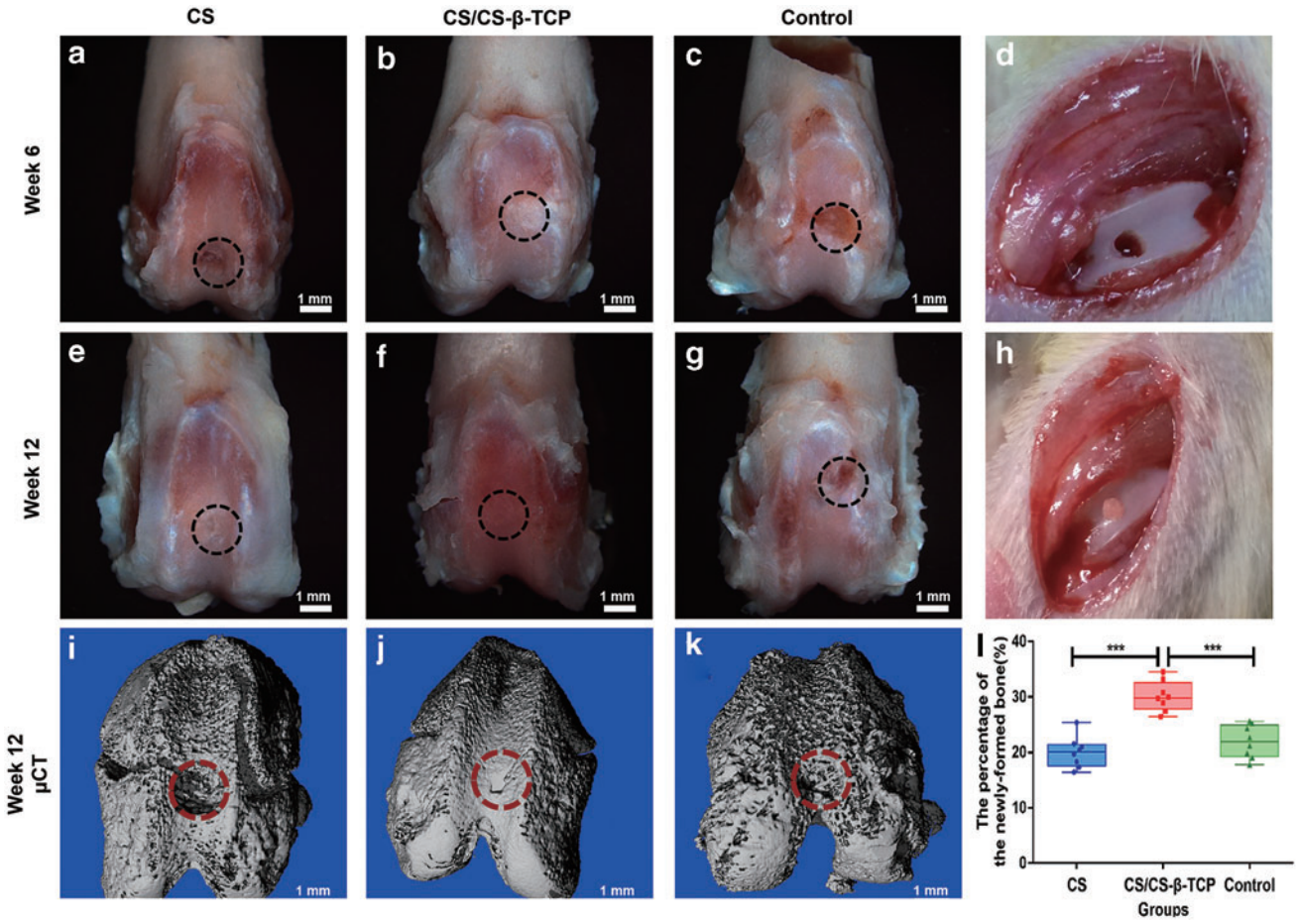


**Figure 5.** Macroscopic photographs of the defect sites in the CS, CS/CS-$\beta$-TCP, and blank control group at 6 weeks **(a, e, i)** and 12 weeks **(b, f, j)** after operation. Micro-CT images of the defect sites in the CS **(c)**, CS/CS-$\beta$-TCP **(g)**, and blank control group **(k)** at 12 weeks after operation. **(d)** Shows the osteochondral defect. **(h)** Shows the scaffold implanted into the defect. The percentage of newly formed bone was calculated **(l)**. The *black* and *red dashed circles* show the defect area of the osteochondral defect. Data represent mean ± standard deviation; ***$p < 0.001$. CT, computed tomography. Color images are available online.

## Histological examination

The histological examination was further performed by HE and Masson staining. At 6 weeks after operation, in the CS group, the cartilaginous defects were partially repaired with some collagen filled in it (Fig. 6a, b). The subchondral defects were completely unrepaired. Moreover, a large amount of residual scaffolds were still observed in the defect sites (Fig. 6a, b). As to the defect sites covered by the CS/CS-$\beta$-TCP scaffold, some amount of the cartilage-like tissues was formed and the surface of the defects was smooth (Fig. 6e, f). Moreover, some cancellous bone was formed in the subchondral layer of the defects. Although the newly formed cartilage was still thinner compared with the normal cartilage, still some residual scaffolds existed in the defect sites (Fig. 6e, f). As to the blank control group, the defects were still unfilled, and only some fibrous tissues were observed in the bottom of the defects (Fig. 6i, j).

At 12 weeks after operation, the osteochondral defect in the blank group was still unrepaired although a small amount of cancellous bone was formed (Fig. 6k, l). In the CS group, an incompletely repaired defect with a larger amount of the cartilage-like tissue was observed when compared with that of the blank control group (Fig. 6c, d).

**Table 3.** *Results of macroscopic grading scale*

| *Grading* | *Control Group* | *CS Group* | *CS/CS-β-TCP Group* |
|---|---|---|---|
| Coverage | 0.79 ± 0.35 | 2.54 ± 0.25[a] | 3.88 ± 0.17[a,b] |
| Neocartilage color | 0.88 ± 0.43 | 1.88 ± 0.17[a] | 3.88 ± 0.17[a,b] |
| Margins | 0.96 ± 0.28 | 1.84 ± 0.18[a] | 3.67 ± 0.18[a,b] |
| Surface | 0.71 ± 0.38 | 0.84 ± 0.18 | 3.79 ± 0.17[a,b] |
| Total | 3.34 ± 0.69 | 7.09 ± 0.49[a] | 15.22 ± 0.35[a,b] |

Each set of data represents the mean and standard deviation of the scales.
[a]$p \leq 0.05$, versus control group.
[b]$p \leq 0.05$, versus CS group.
CS, chitosan.

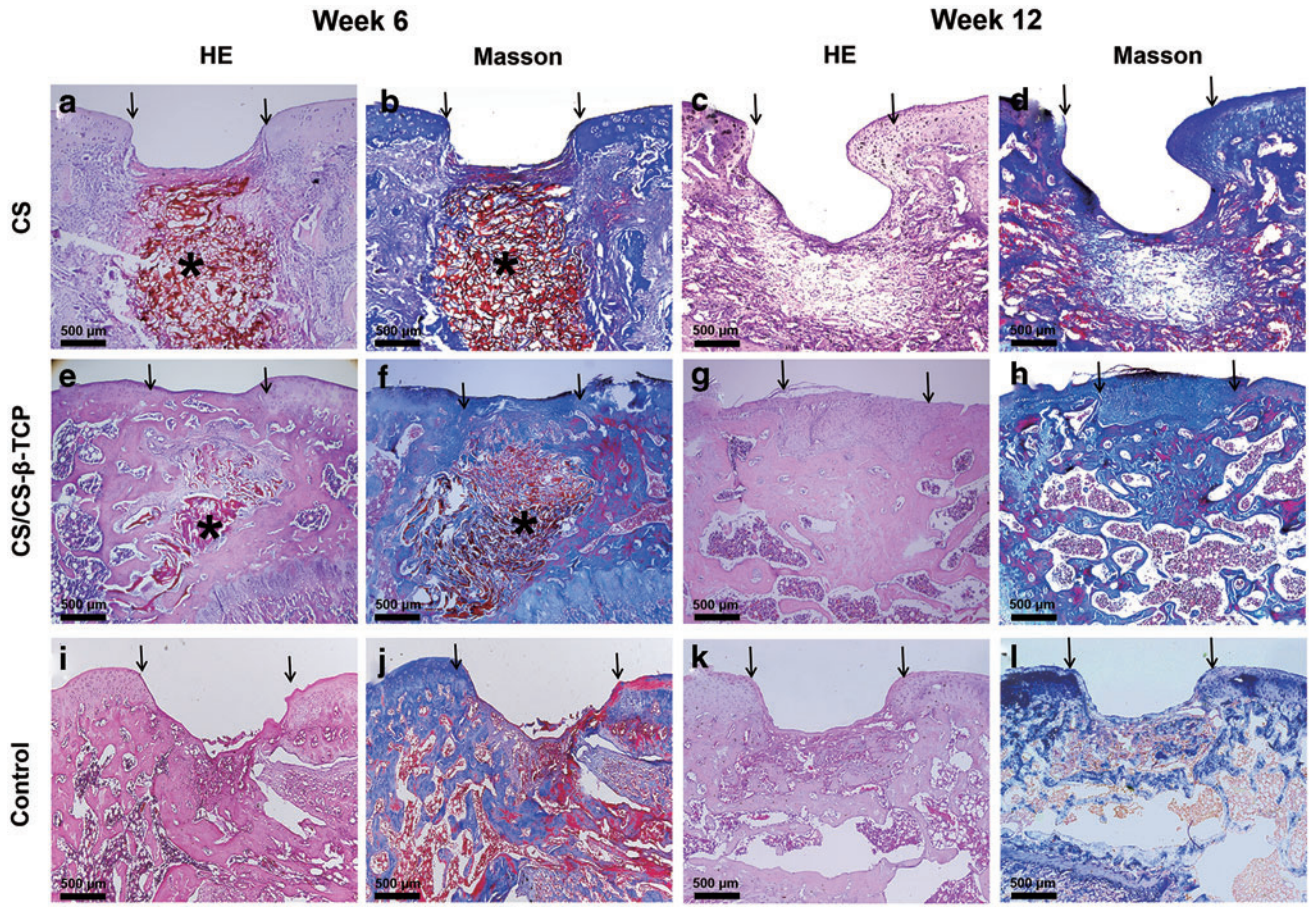


**Figure 6.** HE and Masson staining of the defect sites in the CS, CS/CS-$\beta$-TCP, and blank control group at 6 weeks **(a, b, e, f, i, j)** and 12 weeks **(c, d, g, h, k, l)** after operation. The *arrows* showed the edges of the defects. The "*" showed the residual scaffolds **(a, b, d, e)**. Scale bars = 500 $\mu$m. HE, hematoxylin and eosin. Color images are available online.

Fibrous tissues, rather than bone-like tissues were filled in the deep regions of the defects (Fig. 6c, d). As to the CS/CS-$\beta$-TCP group, the newly formed bone tissues were formed in the deep site, and a limit amount of cartilaginous tissues were formed on the surface of the osteochondral defects. Moreover, the thickness of the newly formed cartilaginous tissues was a little thicker than that of the native cartilage (Fig. 6g, h). Some residual scaffold materials can still be observed in defect sites of the CS group (Fig. 6c, d). The result of the ICRS Visual Histological Assessment Scale of the three groups is shown in Table 4; the total score of the bi-layered CS/CS-$\beta$-TCP group was significantly higher than that of the mono-layered CS group ($p < 0.05$) and blank group ($p < 0.05$).

### Immunohistochemical examination

Immunohistochemical examination of Col-I and Col-II was further performed in CS and CS/CS-$\beta$-TCP groups. At 6 weeks after the operation, expression of Col-II was observed on the surface region of the defect sites in both CS and CS/CS-$\beta$-TCP groups (Fig. 7b, f). At 12 weeks after operation, the expression of Col-II was observed in the newly formed cartilage of the CS/CS-$\beta$-TCP group (Fig. 7h). However, almost no expression of Col-II was observed in the defect sits of the CS groups (Fig. 7d). During the whole healing process, Col-I was positively expressed in the subchondral osseous

**Table 4.** *Results of International Cartilage Repair Society Visual Histological Assessment Scale*

| *Subchondral bone* | *Subchondral bone* | *Subchondral bone* | *Subchondral bone* |
|---|---|---|---|
| Surface | 0.88 ± 1.06 | 0.75 ± 0.71 | 2.88 ± 0.35[a,b] |
| Matrix | 1.00 ± 0.62 | 1.38 ± 0.45 | 2.67 ± 0.18[a,b] |
| Cell distribution | 1.68 ± 0.46 | 1.71 ± 0.45 | 2.54 ± 0.18[a,b] |
| Viability of cell population | 2.67 ± 0.71 | 2.83 ± 0.47 | 2.92 ± 0.24 |
| Subchondral bone | 2.42 ± 0.30 | 1.46 ± 0.25[a] | 2.50 ± 0.18[b] |
| Total | 8.64 ± 2.28 | 9.13 ± 1.40 | 13.50 ± 0.51[a,b] |

Each set of data represents the mean and standard deviation of the scales.
[a] $p \leq 0.05$, versus control group.
[b] $p \leq 0.05$, versus CS group.

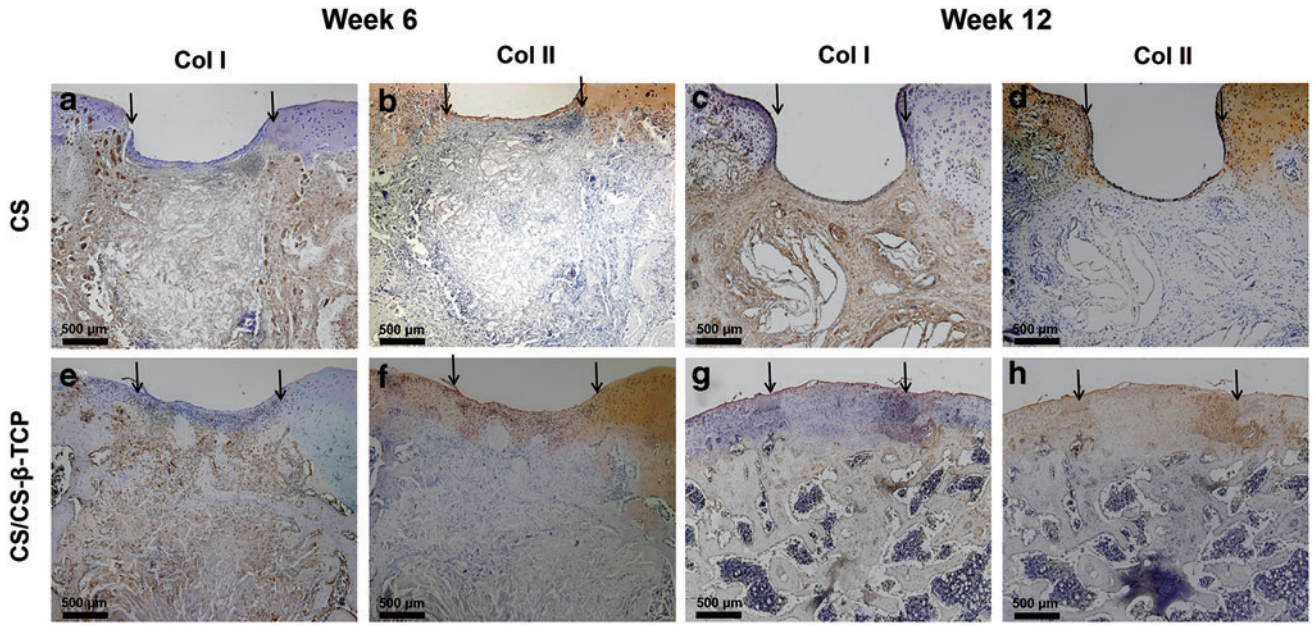


**Figure 7.** Immumohistochemical staining of Col-I and Col-II in the CS and CS/CS-$\beta$-TCP group at 6 weeks **(a, b, e, f)** and 12 weeks **(c, d, g, h)** after operation. The *arrows* showed the edges of the defects. Scale bars = 500 $\mu$m. Color images are available online.

tissue of the defect sites but negatively expressed in the cartilaginous tissue (Fig. 7a, c, e, g).

## DISCUSSION

An ideal scaffold for osteochondral defect repair should include two layers: cartilage and bone layers. The cartilage layer should provide a 3D structure to facilitate attachment and proliferation of chondrocytes and promote regeneration of cartilage. In the meantime, scaffolds that are used for bone layers should withhold skeleton stress and facilitate the synthesis of osteogenic differentiation factors. Recent studies have mentioned several kinds of bi-layered scaffolds and their usage in the treatment of osteochondral defects.[12,14,33] However, the fabrication technologies of pressing method[14] and suturing methods[33] were expensive and difficult to operate. The interface between two layers created by the earlier mentioned fabrication methods was not a natural transition and easily to be detached.

In this study, an easily prepared bi-layered CS/CS-$\beta$-TCP scaffold for osteochondral defect repair was fabricated by using the freeze-drying technique. The immunofluorescence positive staining of Col-II (Fig. 4a, b) and negative staining of Col-I (Fig. 4c, d) indicated that chondrocytes seeded in the CS layer maintained the chondrogenic lineage and produced the chondrogenic factors. Moreover, BMSCs in the CS-$\beta$-TCP layer differentiated into the osteogenic lineage and expressed a large amount of OCN (Fig. 4e, f) and Col-I (Fig. 4g, h). These demonstrated that both cartilage and bone layers can play their distinctive roles in the regeneration processes of the osteochondral defects.

In the bi-layered CS/CS-$\beta$-TCP scaffold, CS forms the base material for each of the layers of this bi-layered construct, thus offering the advantage of the presence of natural binding sites that connect the two layers into an integral whole. Incorporation of $\beta$-TCP into CS scaffold can increase the mechanical properties of the composite scaffold.[35] The pore size of the CS layer of the scaffolds was 120–400 $\mu$m (Fig. 2d) and the porosity was 75.3% $\pm$ 2.4%, which was suitable for chondrocyte proliferation and ECM formation.[36] Incorporation of $\beta$-TCP decreases the pore size (10–80 $\mu$m) of the composite scaffold (Fig. 2e). From the results of *in vitro* and *in vivo* experiments (Figs. 3d–f, 4e–h, and 5g), the CS-$\beta$-TCP layer with a pore size of 10–80 $\mu$m was suitable for the proliferation and differentiation of BMSCs and new bone formation.[35]

From the results of Micro-CT (Fig. 5c, g, k) and histological examination (Fig. 6), the CS/CS-$\beta$-TCP bi-layered scaffold exhibits a better repair effect to the osteochondral defects when compared with that of the CS scaffold. This may due to the osteogenic ability of the CS-$\beta$-TCP layer, as it is capable of promoting attachment and osteogenesis of BMSCs.[26] From the results of histological examination (Fig. 6c, g), the defects treated by the

bi-layer scaffold were filled with the newly formed bone, whereas the defects treated by the CS scaffold were incompletely filled. The newly formed bone can provide not only a skeleton but also a favorable mechanical environment for the regeneration of cartilage above them.[33,37] Therefore, the amount of the newly formed cartilage in the CS/CS-$\beta$-TCP group is also larger than that of the CS group and even exhibits a similar structure with the native cartilage (Fig. 6g, h). The regeneration of the cartilaginous tissue was faster in the CS/CS-$\beta$-TCP group compared with that of the CS group (Fig. 6b, f).

**KEY FINDINGS**

- The bi-layered composite CS/CS-$\beta$-TCP scaffold exhibits a hierarchical structure.
- The seeded chondrocytes in the CS layer could maintain the chondrogenic lineage, whereas BMSCs in the CS-$\beta$-TCP layer could continually differentiate into the osteogenic lineage cells.
- A better repair effect was achieved in the osteochondral defects treated by the bi-layered CS/CS-$\beta$-TCP scaffold than that of the mono-layered CS scaffold.

The replacement of the scaffolds by newly formed tissues in the defects treated by the CS/CS-$\beta$-TCP bi-layered scaffolds was also faster than that of the CS group. At 6 weeks after operation, a large amount of the residual scaffolds could be observed in the defect sites of the CS group, whereas only a few residual scaffold materials were found in the defect sites of the CS/CS-$\beta$-TCP groups (Fig. 6a, e). These results demonstrate that a fast degradation rate of the residual scaffolds caused by the CS/CS-$\beta$-TCP scaffold might accelerate the process of osteogenesis.[38]

The normal articular surface is covered with hyaline cartilage containing Col-II, and the cartilage is tightly bonded with the subchondral bone containing Col-I.[39] For the mono-layered CS group, only a small amount of Col-II was observed in the surface area of the repair tissue at 6 weeks after operation (Fig. 7b), but it was not detected at 12 weeks after operation (Fig. 7d). These results indicated that almost no cartilaginous tissue was produced in the defect sites of the CS group during the entire process of healing. On the contrary, the newly formed tissues in the defect sites of the CS/CS-$\beta$-TCP group all expressed the positive immunohistochemical staining of Col-II (Fig. 7f, h), which indicated that the regenerated tissues were cartilaginous tissues.

Immunohistochemical staining of Col-I was used to indicate the fibrocartilages and subchondral bone tissues. The subchondral areas in the defect sites of both CS and CS/CS-$\beta$-TCP groups expressed a positive staining of Col-I during the entire healing process (Fig. 7a, c, e, g), which means that the subchondral bone tissues are successfully regenerated under the help of CS and CS/CS-$\beta$-TCP scaffolds. It also means that bone tissues are more easily regenerated than cartilage, as cartilage tissues lack vessels and nutrition supply.[2] The cartilaginous tissues of the CS/CS-$\beta$-TCP group were negatively stained by Col-I (Fig. 7e, g), which indicated that the regenerated cartilaginous tissues were hyaline cartilages, rather than fibrocartilages. Moreover, positive expression of Col-I was observed in the subchondral area of the CS/CS-$\beta$-TCP group (Fig. 7g), which demonstrated that new bone formation was successfully achieved by the CS/CS-$\beta$-TCP scaffold.

It should be noted that there are obvious limitations in planning human clinical trials by *in vivo* results that were obtained from the rat model, although rats have already been utilized for the establishment of osteochondral trauma models.[15,30] It is important to follow up successful rats experiments by scaling up and using large animal models. Large animals, such as goats, sheep, pigs, and horses, have comparable joint dimensions and joint load with humans.[40] In consideration of logistic, financial, and ethical requirements, large animal experiments would be performed in future studies.

The bi-layered CS/CS-$\beta$-TCP scaffolds fabricated in this study possess a well biocompatibility. They can not only promote cell proliferation and osteogenic differentiation of BMSCs but also facilitate the regeneration of the osteochondral tissues. In consideration of the excellent performance in clinics and commercial usage of both CS and $\beta$-TCP, the bi-layered CS/CS-$\beta$-TCP scaffold might be an alternative approach for osteochondral defect repair.

## INNOVATION

The treatment of osteochondral defects is a great challenge, because the defects involve the articular cartilage and the subchondral bone. The innovation in this study lies in the designation of the bi-layered composite CS/CS-$\beta$-TCP scaffold and in the simple and economical fabrication method. The bi-layered scaffold with different biological and mechanical properties of each layer can mimic the hierarchical structures of the native osteochondral tissues. Using the bi-layered CS/CS-$\beta$-TCP scaffold might be an alternative

strategy for the treatment of osteochondral defects according to the results of this study.

## ACKNOWLEDGMENTS AND FUNDING SOURCES

This work was mainly supported by the Fundamental Research Fund for the Central Universities of China (No. 2042017kf0206) and the Scientific Research Project of the Health and Family Planning Commission of Hubei Province (WJ2017M047), and it was partially supported by the Natural Science Foundation of China (No. 81800943) and the Basic Science Research Project of Wenzhou Science and Technology Bureau (Y20180698).

## AUTHOR DISCLOSURE AND GHOSTWRITING

No competing financial interests exist in this study. The content of this article was expressly written by the authors listed, and no ghostwriters were used.

## ABOUT THE AUTHORS

**Dongdong Xu, MD,** is a surgeon in the Department of Oral and Maxillofacial Surgery, School and Hospital of Stomatology, Wenzhou Medical University, Wenzhou, China. **Gu Cheng, PhD,** is a surgeon in the Department of Oral and Maxillofacial Surgery, School and Hospital of Stomatology, Wuhan University, Wuhan, China. **Jinhong Dai, MD,** is a surgeon in the Department of Oral and Maxillofacial Surgery, School and Hospital of Stomatology, Wenzhou Medical University, Wenzhou, China. **Zhi Li, PhD,** is an associate professor in the Department of Oral and Maxillofacial Surgery, School and Hospital of Stomatology, Wuhan University, Wuhan, China.

## REFERENCES

1. Glyn-Jones S, Palmer AJR, Agricola R, et al. Osteoarthritis. Lancet 2015;386:376–387.
2. Lopa S, Madry H. Bioinspired scaffolds for osteochondral regeneration. Tissue Eng Part A 2014; 20:2052–2076.
3. Canata GL, Casale V. Arthroscopic debridement and bone marrow stimulation for talar osteochondral lesions: current concepts. J ISAKOS 2017;2:2–7.
4. Philipp D, Alwina B, Georg B. Postoperative changes in in vivo measured friction in total hip joint prosthesis during walking. PLoS One 2015; 10:e0120438.
5. Haene R, Qamirani E, Story RA, Pinsker E, Daniels TR. Intermediate outcomes of fresh talar osteochondral allografts for treatment of large osteochondral lesions of the talus. J Bone Joint Surg Am Vol 2012;83-A:1285.
6. Shimozono Y, Hurley ET, Myerson CL, Kennedy JG. Good clinical and functional outcomes at midterm following autologous osteochondral transplantation for osteochondral lesions of the talus. Knee Surg Sports Traumatol Arthrosc 2018;26: 3055–3062.
7. Hangody LR, Gál T, Szűcs A, et al. Osteochondral allograft transplantation from a living donor. Arthroscopy 2012;28:1180–1183.
8. Ross KA, Robbins J, Easley ME, Kennedy JG. Bone marrow stimulation and biological adjuncts for treatment of osteochondral lesions of the talus. Tech Foot Ankle Surg 2015;14:41–52.
9. Enea D, Cecconi S, Calcagno S, Busilacchi A, Manzotti S, Gigante A. One-step cartilage repair in the knee: Collagen-covered microfracture and autologous bone marrow concentrate. A pilot study. Knee 2015;22:30–35.
10. Steinwachs MR, Waibl B, Mumme M. Arthroscopic treatment of cartilage lesions with microfracture and BST-CarGel. Arthrosc Tech 2014;3: e399–e402.
11. Li X, Ding J, Wang J, Zhuang X, Chen X. Biomimetic biphasic scaffolds for osteochondral defect repair. Regen Biomater 2015;2:221–228.
12. Galperin A, Oldinski RA, Florczyk SJ, Bryers JD, Zhang M, Ratner BD. Integrated bi-layered scaffold for osteochondral tissue engineering. Adv Healthc Mater 2013;2:872–883.
13. Zhang S, Chen L, Jiang Y, et al. Bi-layer collagen/microporous electrospun nanofiber scaffold improves the osteochondral regeneration. Acta Biomater 2013;9:7236–7247.
14. Kim SH, Kim SH, Jung Y. Bi-layered PLCL/(PLGA/$\beta$-TCP) composite scaffold for osteochondral tissue engineering. J Bioact Compat Polym 2015;30: 178–187.
15. Hu X, Wang Y, Tan Y, et al. A difunctional regeneration scaffold for knee repair based on Aptamer-directed cell recruitment. Adv Mater 2017;29:1605235.
16. Scaffaro R, Lopresti F, Botta L, Rigogliuso S, Ghersi G. Integration of PCL and PLA in a monolithic porous scaffold for interface tissue engineering. J Mech Behav Biomed Mater 2016;63: 303–313.
17. Ávila HM, Feldmann EM, Pleumeekers MM, et al. Novel bilayer bacterial nanocellulose scaffold supports neocartilage formation in vitro and in vivo. Biomaterials 2015;44:122–133.
18. Kean T, Thanou M. Biodegradation, biodistribution and toxicity of chitosan. Adv Drug Deliver Rev 2010;62:3–11.
19. Ahmed S, Ikram S. Chitosan based scaffolds and their applications in wound healing. Achievements Life Sci 2016;10:27–37.
20. Pezeshki-Modaress M, Rajabi-Zeleti S, Zandi M, et al. Cell-loaded gelatin/chitosan scaffolds fabricated by salt-leaching/lyophilization for skin tissue engineering: In vitro and in vivo study. J Biomed Mater Res A 2014;102:3908–3917.
21. Choi B, Kim S, Lin B, Wu BM, Lee M. Cartilaginous extracellular matrix-modified chitosan hydrogels for cartilage tissue engineering. Acs Appl Mater Interfaces 2014;6:20110–20121.
22. Lahiji A, Sohrabi A, Hungerford DS, Frondoza CG. Chitosan supports the expression of extracellular matrix proteins in human osteoblasts and chondrocytes. J Biomed Mater Res 2015;51:586–595.
23. Nettles DL, Elder SH, Gilbert JA. Potential use of chitosan as a cell scaffold material for cartilage tissue engineering. Tissue Eng Part A 2002;8: 1009–1016.
24. Dessì M, Borzacchiello A, Mohamed TH, Abdel-Fattah WI, Ambrosio L. Novel biomimetic thermosensitive $\beta$-tricalcium phosphate/chitosan-based hydrogels for bone tissue engineering. J Biomed Mater Res A 2013;101:2984–2993.
25. Serra IR, Fradique R, Vallejo MCS, Correia TR, Miguel SP, Correia IJ. Production and characterization of chitosan/gelatin/$\beta$-TCP scaffolds for

improved bone tissue regeneration. Mater Sci Eng C 2015;55:592–604.

26. Wang J, Jiang B, Guo W, Zhao Y. Indirect 3D printing technology for the fabrication of customised $\beta$-TCP/chitosan scaffold with the shape of rabbit radial head-an in vitro study. J Orthop Surg Res 2019;14:102.
27. Moreau JL, Xu HHK. Mesenchymal stem cell proliferation and differentiation on an injectable calcium phosphate—Chitosan composite scaffold. Biomaterials 2009;30:2675–2682.
28. Zhang R, Ma PX. Poly(alpha-hydroxyl acids)/hydroxyapatite porous composites for bone-tissue engineering. I. Preparation and morphology. J Biomed Mater Res 2015;44:446–455.
29. Du G, Song Y, Wei L, et al. Osthole inhibits proliferation and induces catabolism in rat chondrocytes and cartilage tissue. Cell Physiol Biochem 2015;36:2480–2493.
30. Xue D, Zheng Q, Zong C, et al. Osteochondral repair using porous poly(lactide-co-glycolide)/nano-hydroxyapatite hybrid scaffolds with undifferentiated mesenchymal stem cells in a rat model. J Biomed Mater Res A 2010;94A:259–270.
31. Sun X, Su W, Ma X, Zhang H, Sun Z, Li X. Comparison of the osteogenic capability of rat bone mesenchymal stem cells on collagen, collagen/hydroxyapatite, hydroxyapatite and biphasic calcium phosphate. Regen Biomater 2018;5:93–103.
32. Li X, Jin L, Balian G, Laurencin CT, Anderson DG. Demineralized bone matrix gelatin as scaffold for osteochondral tissue engineering. Biomaterials 2006;27:2426–2433.
33. Cui W, Wang Q, Gang C, et al. Repair of articular cartilage defects with tissue-engineered osteochondral composites in pigs. J Biosci Bioeng 2011;111:493–500.
34. Cheng G, Chen X, Li Z, Lu H, Davide O, Li Z. Comparison of three inoculation methods for bone tissue engineering. Int J Oral Maxillofac Implants 2012;27:1340–1350.
35. Kucharska M, Butruk B, Walenko K, Brynk T, Ciach T. Fabrication of in-situ foamed chitosan/$\beta$-TCP scaffolds for bone tissue engineering application. Mater Lett 2012;85:124–127.
36. Lien SM, Ko LY, Huang TJ. Effect of pore size on ECM secretion and cell growth in gelatin scaffold for articular cartilage tissue engineering. Acta Biomater 2009;5:670–679.
37. Petersen JP, Ueblacker P, Goepfert C, et al. Long term results after implantation of tissue engineered cartilage for the treatment of osteochondral lesions in a minipig model. J Mater Sci Mater Med 2008;19:2029–2038.
38. Azevedo AS, Sá MJC, Fook MVL, et al. Use of chitosan and $\beta$-tricalcium phosphate, alone and in combination, for bone healing in rabbits. J Mater Sci Mater Med 2014;25:481–486.
39. Tatebe M, Nakamura R, Kagami H, Okada K, Ueda M. Differentiation of transplanted mesenchymal stem cells in a large osteochondral defect in rabbit. Cytotherapy 2005;7:520–530.
40. Schneider-Wald B, Thaden A, Schwarz M. Defect models for the regeneration of articular cartilage in large animals [in German]. Orthopde 2013;42:242.

**Abbreviations and Acronyms**

$\beta$-TCP = $\beta$-tricalcium phosphate
BMSCs = bone marrow stem cells
CFSE = 5,6-carboxyfluorescein diacetate, succinimidyl ester
CLSM = confocal laser scanning microscopy
CM-DiI = 3*H*-Indolium,5-[[[4-(chloromethyl)benzoyl]amino]methyl]-2-[3-(1,3-dihydro-3,3-dimethyl-1-octadecyl-2*H*-indol-2-ylidene)-1-propenyl]-3,3-dimethyl-1-octadecyl-, chloride
Col-I = type I collagen
Col-II = type II collagen
CS = chitosan
CT = computed tomography
DMEM/F12 = Dulbecco's modified Eagle medium/Nutrient Mixture Ham-12
ECM = extracellular matrix
EDTA = ethylenediaminetetraacetic acid
FBS = fetal bovine serum
HE = hematoxylin and eosin
ICRS = International Cartilage Repair Society
OCN = osteocalcin
PBS = phosphate-buffer solution
PLCL = poly(lactide-*co*-glycolide)
PLGA = poly(lactic-*co*-glycolic acid)
P-S = penicillin–streptomycin
SD = Sprague-Dawley
SEM = scanning electron microscope